NEURAL REGENERATION RESEARCH
www.nrronline.org

Research Article

Silencing the enhancer of zeste homologue 2, *Ezh2*, represses axon regeneration of dorsal root ganglion neurons

https://doi.org/10.4103/1673-5374.330623
Date of submission: April 20, 2021
Date of decision: May 12, 2021
Date of acceptance: August 6, 2021
Date of web publication: December 10, 2021

Ting-Ting Guo[1], Ying Zhao[1], Wei-Xiao Huang[1], Tao Zhang[1], Li-Li Zhao[1, 2], Xiao-Song Gu[1, *], Song-Lin Zhou[1, *]

From the Contents

Graphical Abstract

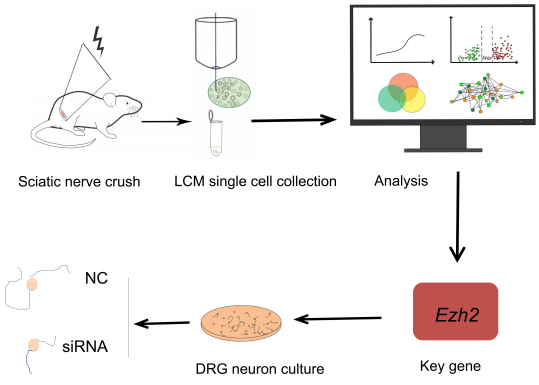

Abstract

Recovery from injury to the peripheral nervous system is different from that of the central nervous system in that it can lead to gene reprogramming that can induce the expression of a series of regeneration-associated genes. This eventually leads to axonal regeneration of injured neurons. Although some regeneration-related genes have been identified, the regulatory network underlying axon regeneration remains largely unknown. To explore the regulator of axon regeneration, we performed RNA sequencing of lumbar L4 and L5 dorsal root ganglion (DRG) neurons at different time points (0, 3, 6, 12 hours, 1, 3 and 7 days) after rat sciatic nerve crush. The isolation of neurons was carried out by laser capture microscopy combined with NeuN immunofluorescence staining. We found 1228 differentially expressed genes in the injured sciatic nerve tissue. The hub genes within these differentially expressed genes include *Atf3*, *Jun*, *Myc*, *Ngf*, *Fgf2*, *Ezh2*, *Gfap* and *Il6*. We verified that the expression of the enhancer of zeste homologue 2 gene (*Ezh2*) was up-regulated in DRG neurons after injury, and this up-regulation differed between large- and small-sized dorsal root ganglion neurons. To investigate whether the up-regulation of *Ezh2* impacts axonal regeneration, we silenced *Ezh2* with siRNA in cultured DRG neurons and found that the growth of the newborn axons was repressed. In our investigation into the regulatory network of Ezh2 by interpretive phenomenal analysis, we found some regulators of *Ezh2* (including *Erk*, *Il6* and *Hif1a*) and targets (including *Atf3*, *Cdkn1a* and *Smad1*). Our findings suggest that *Ezh2*, as a nerve regeneration-related gene, participates in the repair of the injured DRG neurons, and knocking down the *Ezh2 in vitro* inhibits the axonal growth of DRG neurons. All the experimental procedures approved by the Administration Committee of Experimental Animals of Jiangsu Province of China (approval No. S20191201-201) on March 21, 2019.

Key Words: axon regeneration; dorsal root ganglion neurons; *Ezh2*; IB4; laser capture microscopy; NF160/200; quantitative reverse transcription-polymerase chain reaction; sciatic nerve crush; scRNA-seq; siRNA

Chinese Library Classification No. R459.9; R363; R364

Introduction

Although the peripheral nervous system has some ability of self-regeneration and repair after injury, the effect of such repair is not ideal (Gu et al., 2020; Yang et al., 2020; Li et al., 2021). At present, the main clinical treatments are direct nerve repair, nerve transplantation, nerve transfer, fibrin glue, nerve conduit, cell therapy, drugs and electrical nerve stimulation (Hussain et al., 2020). Dorsal root ganglions (DRGs) are a group of cell bodies responsible for transmitting sensory information from receptors such as heat receptors,

[1]Key Laboratory of Neuroregeneration of Jiangsu and Ministry of Education, NMPA Key Laboratory for Research and Evaluation of Tissue Engineering Technology Products, Jiangsu Clinical Medicine Center of Tissue Engineering and Nerve Injury Repair, Co-Innovation Center of Neuroregeneration, Nantong University, Nantong, Jiangsu Province, China; [2]Model Animal Research Center and MOE Key Laboratory of Animal Models of Disease, Nanjing University, Nanjing, Jiangsu Province, China

*Correspondence to: Xiao-Song Gu, PhD, nervegu@ntu.edu.cn; Song-Lin Zhou, PhD, songlin.zhou@ntu.edu.cn.
https://orcid.org/0000-0002-2562-6275 (Xiao-Song Gu); https://orcid.org/0000-0001-8598-0922 (Song-Lin Zhou)

Funding: *This study was supported by the National Key Basic Research Program of China, No. 2017YFA0104701 (to XSG); the National Natural Science Foundation of China, No. 31730031 (to XSG), 81870975 (to SLZ); Priority Academic Program Development of Jiangsu Higher Education Institutions (PAPD) (to XSG); the Natural Science Foundation of Jiangsu Province, No. BK20202013 (to XSG).*
How to cite this article: *Guo TT, Zhao Y, Huang WX, Zhang T, Zhao LL, Gu XS, Zhou SL (2022) Silencing the enhancer of zeste homologue 2, Ezh2, represses axon regeneration of dorsal root ganglion neurons. Neural Regen Res 17(7):1518-1525.*

nociceptors, proprioceptors and chemoreceptors to the central nervous system (CNS) in response to a variety of symptoms, such as tingling, burning, numbness or severe pain (Pope et al., 2013). In severe cases, sensory and motor dysfunction and even lifelong disability may occur (Noble et al., 1998). Many studies have shown that macrophages (Zigmond and Echevarria, 2019) and Schwann cells (Poplawski et al., 2018) in the peripheral nervous system play an important role in axonal regeneration during the process of DRG injury repair and that various transcription factors, including *ATF3* and *Smad1*, that promote axon regeneration are part of this process (Zou et al., 2009; Gey et al., 2016).

Enhancer of Zeste Homolog 2 (*Ezh2*) is a methyltransferase that is enthusiastically discussed in the field of cancer as it can either promote carcinogenesis and metastasis or inhibit tumorigenesis. Thus, it has become a target gene during the therapeutic process of many cancers (Chu et al., 2020; Kleer et al., 2003; Mallen-St Clair et al., 2012; Zingg et al., 2015; Gan et al., 2018; Krill et al., 2020). It has also been studied in other fields such as angiogenesis (Tsou et al., 2019), neurodevelopment (Wever et al., 2018) and bone formation (Dudakovic et al., 2018). However, there have been few studies in the peripheral nervous system. There is evidence that knocking down of *Ezh2* affects Schwann cell myelin formation when Schwann cells are co-cultured with DRG neurons (Heinen et al., 2012).

To investigate the expression and function of *Ezh2* in DRG neurons after sciatic nerve injury in a rat model, we examined DRG sections and isolated neurons at seven time periods after sciatic nerve injury and performed RNA-seq and immunofluorescence analysis.

Materials and Methods

Ethics statement

All the experimental procedures involving animals were ethically approved by the Administration Committee of Experimental Animals of Jiangsu Province of China (approval No. S20191201-201) on March 21, 2019 and were used in accordance with Institutional Animal Care guidelines of Nantong University.

Modeling and single cell capture

We used 150 adult Sprague-awley rats weighing 180–220 g in this study. Among them, 56 rats were used for scRNA-seq, 56 rats were used for the *in vivo* experiment (RNA sequencing; RNA extraction; immunofluorescence and immunocytochemistry) and 38 rats were used for the *in vitro* experiment (primer DRG neuron cultures). First, the rats were anesthetized intraperitoneally by an injection of a mixture of 85 mg/kg trichloroacetaldehyde monohydrate (RichJoint, Shanghai, China), 42 mg/kg magnesium sulfate (Xilong Scientific, Guangzhou, China) and 17 mg/kg sodium pentobarbital (Sigma-Aldrich, St. Louis, MO, USA). Under anesthesia, the sciatic nerve was exposed and hemostatic forceps clipped the sciatic nerve for 30 seconds to form a 3-mm transparent section, similar to the crush procedure described by Kalender et al. (2009). Finally, the wound was sutured and wiped with iodophor to avoid wound infection. Normal uninjured rats were used as the control group (0 hour).

After the model was constructed, seven rats were anesthetized as above and sacrificed by neck dislocation at each of the times 0, 3, 6, 12 hours, 1, 3 and 7 days. The L4-L5 DRG was removed and then embedded in O.C.T. compound (Sakura, Torrance, CA, USA) for the frozen sectioning at 12 μm. The sections were dried for 10 minutes in the box containing silica desiccant and then stained with NeuN direct labeled antibody (1:100; Abcam, Cambridge, MA, USA) for 10 minutes. After staining, the sections were rinsed with 0.01 M PBS (Vazym, Nanjing, China) three times, then with diethyl pyrocarbonate (DEPC) water, and dried for 20 minutes. Finally, the DRG neurons were isolated by laser microdissection (Leica, Solms, Germany), during which we cut the target cells close to the boundary of the target cells.

RNA sequencing and data analysis

At 0, 3, 6, 12 hours, 1, 3 and 7 days after modeling, the DRG neurons were collected using laser capture microscopy (LCM) and then dropped into the cell lysis buffer. RNA extraction, reverse transcription, library construction and sequencing were performed according to the manufacturer's protocol (Gene Denovo Biotechnology Co., Guangzhou, China). Briefly, after extracting total RNA from each sample using TRIzol reagent kit (Invitrogen, Carlsbad, CA, USA), Agilent 2100 Bioanalyzer (Agilent Technologies, Palo Alto, CA, USA) was employed for RNA quality control. The samples with high quality were then subjected to mRNA enrichment by Oligo (dT) beads and fragmented with buffers (Gene Denovo Biotechnology Co., Ltd., Guangzhou, China) .

Random primers were used in the reverse transcription from RNA to cDNA, the second-strand cDNA was synthesized by DNA polymerase I, RNase H, dNTP and buffers. Before sequencing, the cDNA fragments were purified with QIAquick PCR extraction kit (Qiagen, Venlo, Netherlands), end-repaired, poly(A) added and finally ligated to Illumina sequencing adapters. The sequencing was carried out using Illumina HiSeq2500 (Gene Denovo Biotechnology Co.).

The raw data from the sequencing machines were further filtered by using filtering of clean reads by Fastp (version 0.18.0), removing ribosome RNA by Bowtie2 (version 2.2.8) (http://bowtie-bio.sourceforge.net/bowtie2), genome mapping using HISAT2.2.4 (http://www.ccb.jhu.edu/software/hisat) and quantification of gene abundance using StringTie (http://ccb.jhu.edu/software/stringtie/). The final measure of gene expression was the fragment per kilobase of transcript per million mapped reads (FPKM) value of each gene in each sample. The expression of differentially expressed genes was analyzed with DESeq2 software between the two different groups. The genes with the parameters of P-value ≤ 0.05 and |log2FC|≥1 were considered as differentially expressed genes (DEGs).

The network of DEGs interaction comes from the String database (https://string-db.org/cgi/input.pl?sessionId=vsDE728IjCfB&input_page_show_search=on). We chose Rattus norvegicus for "Organism" and uploaded the list of DEGs to the website. After the successful load, we hid "disconnected nodes" in the network in the settings before exploring the picture and tables.

RNA extraction

Seven rats were anesthetized then sacrificed by neck dislocation at 0, 3, 6, 12 hours, 1, 3, and 7 days after modeling. The L4–L5 DRG from each rat was taken out and frozen with liquid nitrogen. The tissue/cells were cut up and fully lysed with TRIzol (Vazyme, Guangzhou, China). The samples were then extracted with chloroform on ice for 30 minutes, and the tissue/cells were centrifuged for 30 minutes at 12,000 × g. After addition of isopropanol, the collected supernatant was

incubated at –80°C overnight. The next day, the mixture was centrifuged at 12,000 × *g* for 30 minutes, washed with 75% ethanol, dried, dissolved in DEPC water, and then purified with an organic solvent. The purity and concentration of RNA, dissolved in DEPC, were determined by NanoDrop2000/2000c (Thermo, MA, USA).

Quantitative real-time polymerase chain reaction

After each RNA sample was extracted and its concentration measured, the volume of RNA solution needed for a 1-μg template was calculated and each RNA was reverse transcribed to cDNA by a 2720 Thermal cycler (Applied Biosystems®, UK) with a reverse transcription kit (Vazyme). The quantitative PCR system was prepared with primers, cDNA, and RT-qPCR reverse transcription reagent (Vazyme). The cDNA was diluted three times and then mixed with primer (10 μM, Genscript, Nanjing, China), ChamQ SYBR qPCR Master Mix (High ROX Premixed) (Vazyme) and ddH_2O. Finally, the mixture was put into a LightCycler 96 (Roche, Switzerland) for amplification, the temperature gradient of amplification was as follows: 95°C, 30 seconds, 1 cycle; 95°C, 10 seconds, 60°C, 30 seconds, 40 cycles; 95°C, 15 seconds, 60°C, 60 seconds, 95°C, 15 seconds, 1 cycle. The quantitative method we used was $2^{-\Delta\Delta Ct}$. The relative expression level was calculated using the comparative $2^{-\Delta\Delta Ct}$ method. The primers we used in our study are shown in **Table 1**.

Table 1 | **Primer information**

Gene	Sequence	Product size (bp)
Ezh2	Forward: 5′-CTT TGA TTA CAG ATA CAG CCA GG-3′	23
	Reverse: 5′-AGA ATC AGT TGG TGA TGT TCT GT-3′	23
GAPDH	Forward: 5′-ACG CCA GTA GAC TCC ACG ACA T-3′	22
	Reverse: 5′-CAA CGG GAA ACC CAT CAC CA-3′	20

GAPDH: Glyceraldehyde-3-phosphate dehydrogenase.

Immunofluorescence and immunocytochemistry

The cells were fixed with 4% PFA for 30 minutes, then the cells/tissue sections were washed with PBS for 5 minutes three times at room temperature. The frozen tissue sections were treated with formaldehyde at 0, 3, 6, 12 hours, 1, 3 and 7 days after modeling, then blocked with blocking buffer (Beyotime, Shanghai, China) for 1 hour. Next, the tissue sections were treated with primary antibodies [Ezh2, 1:200, rabbit monoclonal antibody (CST, USA); NF160/200, 1:500, mouse Monoclonal antibody (Sigma-Aldrich); IB4, 1:200, FITC conjugate (Sigma-Aldrich); TuJ1, 1:1 000, mouse monoclonal antibody (Sigma-Aldrich); NeuN, 1: 300, rabbit monoclonal antibody] at 4°C overnight. Eighteen hours later, tissue sections were incubated with secondary antibodies [Cy3-conjugated goat anti-rabbit, 1:500 (Sigma); 488-conjugated goat anti-mouse, 1:500 (Sigma-Aldrich)] for 1.5 hours at room temperature, and then mounted on microscope slides. Finally, an antifade mounting medium with 4,6-diamino-2-phenyl indole (DAPI) solution (Beyotime) was used to seal the slice. Samples were visualized and images captured using an optical and epi-fluorescence microscope (Axio Imager M2, Carl Zeiss Microscopy GmbH, Jena, Germany). All assays were performed in triplicate.

Primer DRG neuron cultures

DRG neurons were primary cultured according to a previous study (Christie et al., 2010). Briefly, the rats were anesthetized by injection of a mixture of 85 mg/kg trichloroacetaldehyde monohydrate, 42 mg/kg magnesium sulfate, and 17 mg/kg sodium pentobarbital. The hair on the back of the rats was removed, then the rats were sacrificed by neck dislocation. The dorsal spinal cord of each rat was quickly separated and the lamina of the spinal cord was opened to facilitate the removal of DRG from the cone hole. The DRG was initially placed in 1% penicillin/streptomycin (Gibco, Carlsbad, CA, USA) in PBS solution on ice. The collected DRGs were washed twice with PBS, treated with 0.5% collagenase (Sigma) for 1.5 hours, and then transferred to 0.25% trypsin (Gibco) for digestion for 25 minutes. When the cell particles were homogeneous, the digestion was terminated with 10% FBS (Gibco) in PBS. The cell particles were washed in 15% BSA PBS and the purified cell precipitate was resuspended by Neurobasal A (Gibco) with 2% B27 (Gibco), 1% penicillin/streptomycin and 1% L-glutamine (Sigma) before being filtered through a sieve (70 μm) into the centrifuge tube for standby. The collected cells were cultured on PLL-coated plates and cultured in an incubator at 37°C in 95% O_2/5% CO_2. Twelve hours later, the culture medium was refreshed with DRG medium containing 10 μM cytosine arabinoside (Cytosine, C21867, Sigma). Neurites from the neurons were observed by their immunoreaction with NeuN 1 day after the cells were planted. The culture medium was refreshed every 3 days.

Small interfering RNA (siRNA) transfection

Primer DRG neurons were transfected with siRNA immediately after planting. The siRNA (RiboBio, China) was diluted to 10 μM with RNase-free water, the mixture of RNAiMax and siRNA transfection was prepared with opti-medium (Gibco) according to the instructions of RNAiMax reagent (Invitrogen). The mixture was incubated at room temperature for 10 minutes and then added to the cell culture medium. The cells were left in an incubator at 37°C in 95% O_2/5% CO_2 for 16 hours. The cells were cultured with complete culture medium without 1% penicillin/streptomycin. The siRNA used in our study is shown in **Table 2**.

Table 2 | **Primer information of small interfering RNA (siRNA) transfection**

Gene	Sequence	Product size (bp)
siRNA-r-Ezh2_001	5′-GGA AAG TGT ATG ACA AAT A-3′	19
siRNA-r-Ezh2_002	5′-GGT AAA TGC TCT TGG TCA A-3′	19
siRNA-r-Ezh2_003	5′-GAG GAA GAC TTC CGA ATA A-3′	19
Negative control-siRNA	5′-GGC UCU AGA AAA GCC UAU GC dTdT-3′ 3′-dTdT CC GAG AUC UUU UCG GAU ACG-3′	44

Fluorescence *in situ* hybridization

The frozen sections were acquired at 0, 3, 6, 12 hours, 1, 3 and 7 days after modeling, as described above, and the slices used for fluorescence *in situ* hybridization (FISH) were kept free of contamination by RNase. All reagents used before tissue slicing were RNase-free, including 4% PFA and dehydrated sucrose solution. Tissue sections were washed twice with 4% DEPC-PFA at room temperature for 5 minutes each, washed twice with PBS at room temperature for 5 minutes each, incubated with 5% DEPC-protein kinase at room temperature for 30 minutes, washed with PBS twice at room temperature for 5 minutes each, fixed with 4% DEPC-PFA at room temperature for 10 minutes, washed with PBS twice at room temperature for 5 minutes each, treated with 0.1 M TEA at room temperature for 10 minutes, washed with

PBS twice at room temperature for 5 minutes each. After incubation in pre-hybridizing solution (RiboBio) at 42°C for 2 hours, tissue sections were hybridized with an Ezh2 probe (Sangon Biotech, Shanghai, China) containing cy5 in the 5′ terminal by hybridizing solution (RiboBio) at 42°C for 12 hours. Then, they were washed with 0.1% Tween-20 4× SSC at 42°C for 10 minutes three times, washed with 2× SSC at 42°C for 10 minutes, with 1× SSC at 42°C for 10 minutes, and with SSC at room temperature for 10 minutes. Finally, tissue sections were washed with PBS for 10 minutes and sealed with antifade mounting medium with DAPI solution (Beyotime). The probe we used is Ezh2 [5′-CAU UGA CAA AAC UUU UCA CAA AAA UUU UGU GCU AUC ACA CAA GGG CAC GAA CUG UCA CAA GGC UGC-3′ (66 bp)].

Statistical analysis

All data were processed using GraphPad prism 8 software (GraphPad Software Inc., San Diego, CA, USA) and are expressed as the mean ± SEM. Repeated measures analysis of variance, one-way analysis of variance followed by the least significant difference *post hoc* test were used for comparison between groups. A level of $P < 0.05$ was considered statistically significant.

Results

The importance of Ezh2 in peripheral nerve injury (PNI) is revealed by scRNA-seq

The DRG cells, harvested after establishing the crush model, were subjected to RNA sequencing by Smart-seq2. The sequence data underwent quality control to obtain clean data. The workflow is shown in **Figure 1A**. Although the number of single DRG neurons obtained by LCM was 100 to 200 at each time point, only 100 repeats at each time point are needed to undergo scRNA-seq2 sequencing.

We obtained the differentially expressed genes (DEGs) by comparing the expression of genes in the injury groups (3, 6, 12 hours, 1, 3 and 7 days) with the normal group (0 hour). A total of 1228 genes showed different expression after injury ($|\log2FC| \geq 1$ and P-value ≤ 0.05), as shown in **Figure 1B**, with red representing up-regulated genes, green representing down-regulated genes and gray representing genes with no significant differences (**Figure 1B**). According to a previous report (Wang et al., 2020), axonal regenerative repair started from 3 days after PNI. From 1 day after the injury, genetic reprogramming was induced intensely and lasted until the 7th day (Renthal et al., 2020). Therefore, the genes with altered expression in each of these three groups may have an important influence on axon regeneration. We found 189 common DEGs by intersection of 391 DEGs at 1 day (0 hour *vs*. 1 day), 795 DEGs at 3 days (0 hour *vs*. 3 days) and 771 DEGs at 7 days (0 hour *vs*. 7 days) (**Figure 1C**).

The interaction between these 189 DEGs was explored with String database. After filtering out the molecules that had no relationship with others, the remained relationships are shown in **Figure 1D**. The molecules in the center of the network present more relationships with others, indicating they may have more influence on this network. The core molecules include a number of cytokines or growth factors, such as *Il6*, *Ngf*, *Fgf2*, *Gfap*, *Cd44*, and *Ccl2*. and transcription factors or regulators such as *Atf3*, *Jun*, *Myc*, *Crem*, *Socs3*, and *Ezh2*.

Ezh2 expression increases in injured DRG neurons and has a difference in large- and small-sized DRG neurons

To investigate the role of Ezh2 in the repair of PNI, we first verified the expression of Ezh2 in DRG neurons. Our scRNA-seq results show that Ezh2 expression consistently increased in L4–5 DRG neurons (**Figure 2A**). Our RT-qPCR, FISH and immunofluorescence experiments showed that Ezh2 expression was consistently increased in injured DRG neurons (**Figure 2B–E**).

In DRG neurons immunofluorescence experiments, we found that the expression of Ezh2 differed in different sizes of DRG neurons. Hu et al. (2016) reported that the heterogeneity of DRG neurons resulted in different sizes of neurons with different sensory functions. Therefore, we labeled DRG neurons by IB4 (small) and NF160/200 (large) (Usoskin et al., 2015). We found that the expression of Ezh2 also increased in large- and small-sized neurons after injury. Moreover, the expression of Ezh2 was different between large- and small-sized neurons, and there were many NF160/200-positive neurons (**Figure 3**). In conclusion, the expression of Ezh2 during the repair of PNI was continuously increased, and the expression of Ezh2 in NF160/200-positive large-sized neurons was high.

The growth of DRG neuron neurites is inhibited by knockdown of Ezh2 *in vitro*

We have shown above that the expression of *Ezh2* in DRG was consistently increased after PNI. To explore the function of *Ezh2* in DRG neurons, we cultured DRG neurons *in vitro*. First, we transfected neurons with siRNA of *Ezh2* and screened the knockdown efficiency of siRNA on *Ezh2* expression (**Figure 4A**), then we stained the neurite of DRG neurons with TuJ1. The staining results indicate that the lengths of neuron neurites in the three groups transfected were significantly shorter than the control group (**Figure 4B**), including the mean length and the longest length (**Figure 4C** and **D**). These results suggest that the knockdown of *Ezh2* expression can inhibit the axonal growth of DRG neurons. Counts of the distribution of neurite lengths showed that the percentage of neurite lengths < 400 μm was significantly higher in *Ezh2*-silenced DRGs than that in the normal control group, whereas the percentage of neurite length > 400 μm was lower in *Ezh2*-silenced DRGs than that in the normal control group (**Figure 4E**). This indicated that the neurite growth was significantly inhibited after silencing *Ezh2*. Finally, we examined the axon growth statistics of DRG neurons after *Ezh2* knockdown in large-sized neurons (surface area > 800 μm^2) and small-sized neurons (surface area < 800 μm^2), which revealed that the neurite growth was significantly suppressed in both (**Figure 4F**). All these results indicate that *Ezh2* is important for DRG neuron regeneration.

Predicting the regulatory network of *Ezh2* involved in axonal growth

Ezh2 is very important for DRG neuron regeneration. Inhibition of *Ezh2* expression inhibits the growth of DRG axons. However, it is not clear how *Ezh2* works or what the possible mechanism and reaction network are. To further search for the regulatory mechanism of *Ezh2* involved in axonal growth, we used Ingenuity Pathway Analysis (IPA) to intersect these molecules with our 1-day *vs*. control differential genes. We found 28 up-regulated regulators and 13 down-regulated effectors of *Ezh2* (**Figure 5**). The different shapes in the graph represent different molecule types. Among the many molecule types, upstream factors such as CASR and MYC have been found to play a role in neuronal axon growth. We hope that the possible upstream and downstream factors of *Ezh2* predicted by us in **Figure 5** will provide the basis for the follow-up studies on PNI repair.

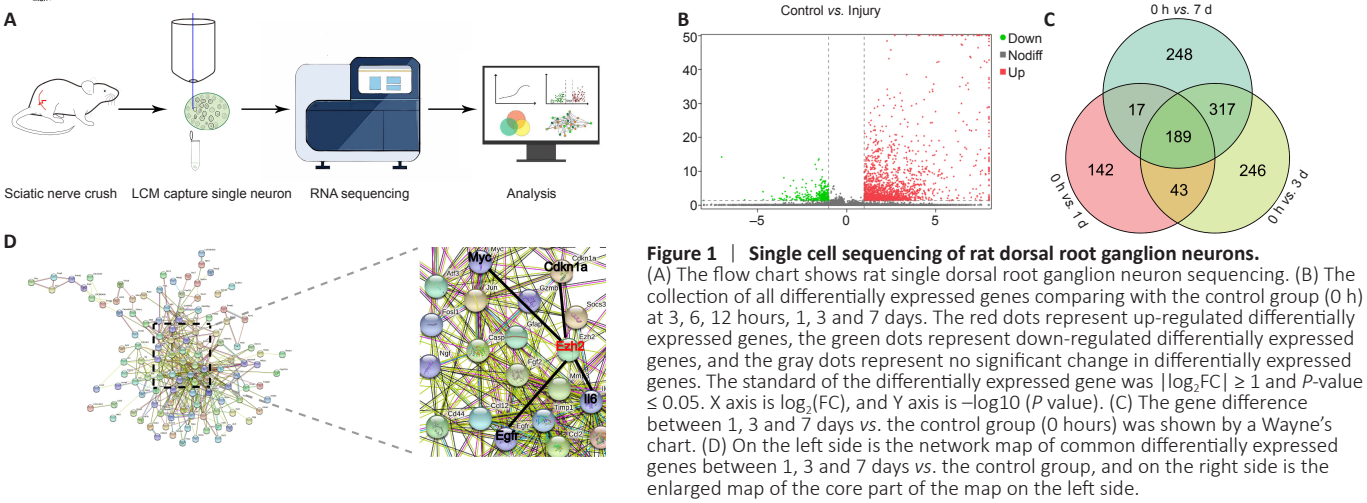

Figure 1 | Single cell sequencing of rat dorsal root ganglion neurons.
(A) The flow chart shows rat single dorsal root ganglion neuron sequencing. (B) The collection of all differentially expressed genes comparing with the control group (0 h) at 3, 6, 12 hours, 1, 3 and 7 days. The red dots represent up-regulated differentially expressed genes, the green dots represent down-regulated differentially expressed genes, and the gray dots represent no significant change in differentially expressed genes. The standard of the differentially expressed gene was $|\log_2 FC| \geq 1$ and *P*-value ≤ 0.05. X axis is $\log_2(FC)$, and Y axis is –log10 (*P* value). (C) The gene difference between 1, 3 and 7 days *vs*. the control group (0 hours) was shown by a Wayne's chart. (D) On the left side is the network map of common differentially expressed genes between 1, 3 and 7 days *vs*. the control group, and on the right side is the enlarged map of the core part of the map on the left side.

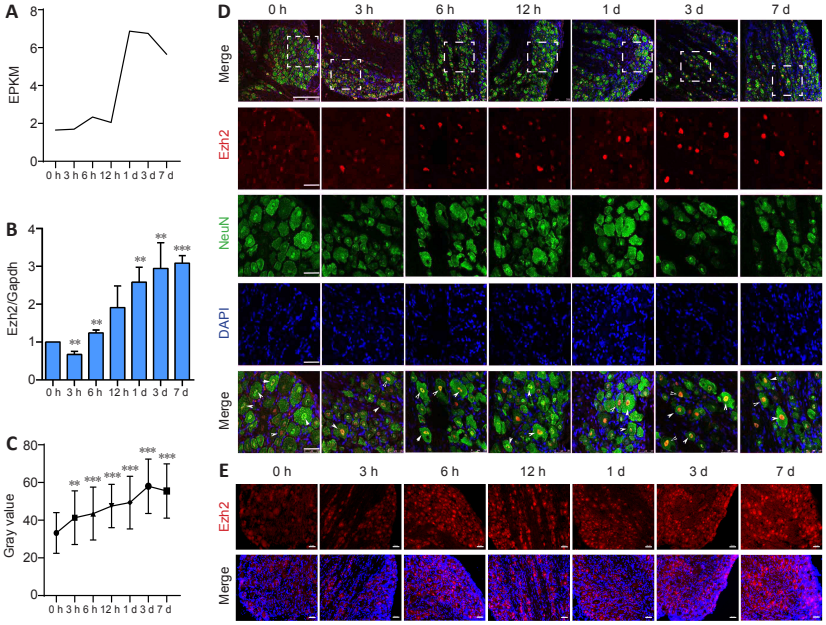

Figure 2 | Expression of Ezh2 in dorsal root ganglion neurons.
(A) Single cell sequencing statistics showed the expression of Ezh2 in dorsal root ganglion neurons after sciatic nerve crush injury. (B) The expression of Ezh2 in dorsal root ganglion neurons after sciatic nerve crush was verified by quantitative reverse transcription-polymerase chain reaction. (C) The quantification of immunostaining of Figure 2D, the vertical axis is mean gray value. (D) The changes of Ezh2 expression in DRG neurons after sciatic nerve crush were verified by immunofluorescence. Red is the Ezh2 marker, green is NeuN neuron specific marker, and blue is the 4,6-diamino-2-phenylindole (DAPI) nuclear marker. In the first row the bar is 250 μm, and in the subsequent rows the bar is 50 μm. The arrow indicates Ezh2 co-labeled with NeuN. (E) Ezh2 probe was used to detect the changing of Ezh2 in dorsal root ganglion neurons after sciatic nerve crush injury. Red represents Ezh2, blue is the DAPI. The experiment was repeated three times. $^{**}P < 0.01$, $^{***}P < 0.001$ (mean ± SEM, $n = 3$, repeated measures analysis of variance). d: Day; FPKM: fragments per kilobase of exon model per million mapped fragments; Gapdh: glyceraldehyde-3-phosphate dehydrogenase; h: hour.

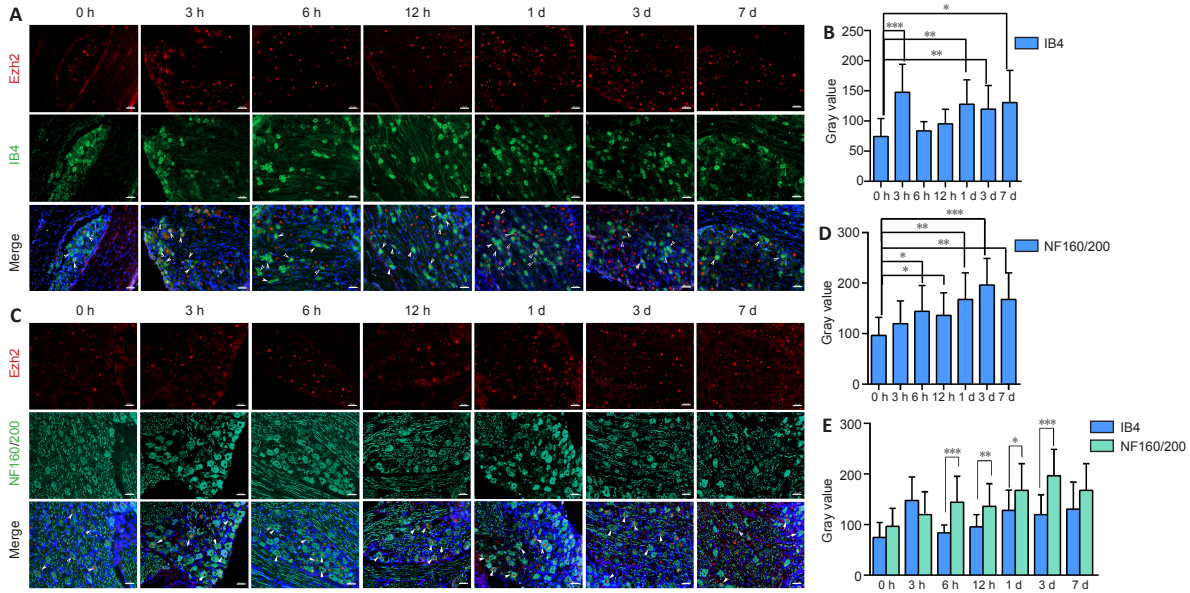

Figure 3 | Expression of Ezh2 in NF160/200- and IB4-positive dorsal root ganglion neurons after sciatic nerve injury.
(A) The expression of Ezh2 in IB4-positive dorsal root ganglion neurons: red is the specific marker of Ezh2, green is the specific marker of IB4, blue is DAPI nuclear marker. Scale bar: 50 μm. (B) The gray value statistical results of Ezh2 expression in IB4-positive dorsal root ganglion neurons. (C) The expression changes of Ezh2 in NF160/200-positive dorsal root ganglion neurons: red is the specific marker of Ezh2, green is the specific marker of NF160/200, and blue is DAPI nuclear marker. Scale bar: 50 μm. (D) The gray value statistical results of Ezh2 expression in NF160/200-positive dorsal root ganglion neurons. (E) The gray value statistical results of the expression difference between NF160/200 and IB4. $^{*}P < 0.05$, $^{**}P < 0.01$, $^{***}P < 0.001$ (mean ± SEM, $n = 3$, repeated measures analysis of variance). The arrows represent Ezh2-IB4 or Ezh2-NF160/200 co-labeled DRG neurons. DAPI: 4,6-Diamino-2-phenyl indole.

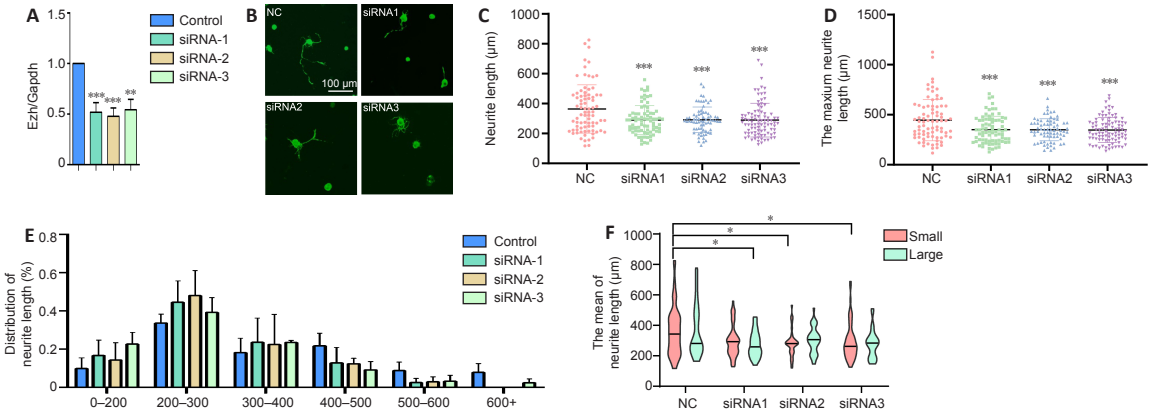

Figure 4 | **Functional verification of Ezh2 in cultured dorsal root ganglion neurons.**
(A) The knockdown efficiency of *Ezh2* by small interfere RNA (siRNA). (B) After siRNA transfection, the axons of the experimental and control groups were stained with *TuJ1*. Scale bar: 100 μm. (C–E) Statistical analysis of the mean and maximum neurite lengths (μm) of dorsal root ganglion neurons in each group after siRNA transfection, and the distribution of neurite lengths in each group. (F) Statistical analysis of the mean neurite length of large-sized neurons (surface area > 800 μm^2) and small-sized neurons (surface area < 800 μm^2) after siRNA transfection. *P < 0.05, **P < 0.01, ***P < 0.001 (mean ± SEM, n = 3, one-way analysis of variance followed by the least significant difference *post hoc* test). NC: Normal control.

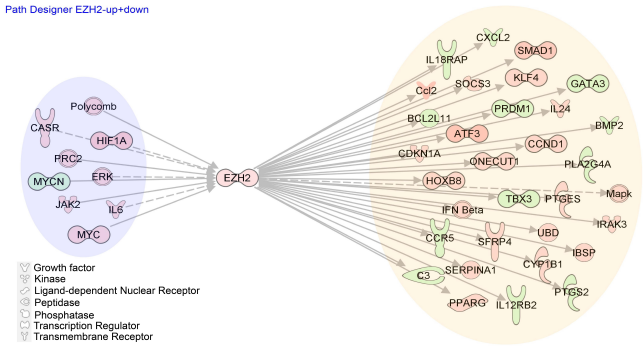

Figure 5 | **Ingenuity pathway analysis predicts the upstream and downstream interaction factors of *Ezh2*.**
On the left is the upstream effector of *Ezh2* in dorsal root ganglion neurons, which is the differentially expressed gene 1 day *vs*. 0 hour after sciatic nerve injury. On the right is the downstream effector. Each arrow indicates an interaction. Pink molecules are up-regulated and green molecules are down-regulated on day 1 *vs*. controls.

Discussion

Analysis of experimental results

After 189 common DEGs were input into the String database, we acquired a molecule interaction net. The functions of most of these molecules, such as Atf3, in neuronal injury or axon regeneration have been reported. The DEG deficient mice show suppression of axons regeneration and function recovery after injury (Renthal et al., 2020). *Ngf* is the normal factor that promotes neuron survival and axon regeneration both *in vivo* and *in vitro* (Oppenheim, 1991). *Il6* and its soluble receptor support the survival of sensory neurons (Thier et al., 1999). Among these core factors, we found that the expression of *Ezh2* in DRG neurons tends to increase after PNI, and interacts with *Myc* (Shin et al., 2021; Whitesides, 2006), *Il-6* (Fischer, 2017), *Cdkn1a* (Utada et al., 2005) and *Egfr* (Stupack et al., 2020) and together these factors regulate axon regeneration. Intrathecal injection of an inhibitor of Ezh2 can alleviate the onset and maintenance of mechanical and thermal hyperalgesia induced by partial sciatic nerve ligation in rats (Yadav and Weng, 2017). It has also been reported that the inhibition of *Ezh2* in DRG neurons under co-culture conditions with Schwann cells leads to disturbance of myelin formation (Heinen et al., 2012). However, there has been no research into the function of *Ezh2* when the sciatic nerve was injured. We found that *Ezh2* expression is up-regulated after neuronal damage and *Ezh2* is at the core of the regulatory network of axonal injury. We demonstrated by RT-qPCR and immunofluorescence staining that there is an upward trend in *Ezh2* expression after sciatic nerve injury. However, we found that inhibition of *Ezh2* expression impeded the axonal growth of DRG neurons. Our results showed that *Ezh2* was differentially expressed in different types of neurons. DRG cells are heterogeneous because they contain different classes of primary sensory neurons, such as pain-associated nociceptive neurons, non-nociceptive temperature sensing and mechanosensory neurons (Haberberger et al., 2020). The heterogeneous populations of sensory neurons in the DRG are subdivided into subclasses based on morphological, neurochemical, electrophysiological and transcriptional characteristics (Platika et al., 1985; Wood et al., 1990; Rugiero and Wood, 2009). There are different subclasses that respond to different physiological and pathological conditions (Zemel et al., 2018). To verify the difference of *Ezh2* expression between large- and small-sized neurons, we chose the classical marker NF160/200 for large-sized neurons and IB4 for small-sized neurons to co-localize with our target molecule Ezh2 (Usoskin et al., 2015). The results showed that *Ezh2* expression was up-regulated in NF160/200-positive DRG neurons after sciatic nerve injury, and there was a difference between NF160/200- and IB4-positive DRG neurons. It has been reported that NF160/200 can be subdivided into C8 subtypes of DRG neurons, which are typical mechanoreceptor neurons (Li et al., 2016). It has been shown that mechanical stimulation can increase the axon growth of large-sized mechanoreceptor neurons and is accompanied up-regulation of the expression of Atf3 (Kampanis et al., 2020). Our *in vitro* experiments showed that the longest neurite length of large-sized neurons was shorter after interference with *Ezh2*. Therefore, whether *Ezh2* can mediate the repair of DRG injury through mechanoreceptor neurons and how *Ezh2* plays a role in it will need further investigation.

Study limitations

The increasing research in single-cell genomics, bioinformatics and computation has brought great benefits to research neuroscience, which not only enables further cellular subtype analysis of neurons and discovery of new neuronal subclasses but also provides a fuller understanding of the molecular expression patterns specific to different types of neurons (Tran et al., 2019). Therefore, we hoped to use scRNA-seq to find breakthrough points in nerve repair. We obtained single cell samples by LCM and chose smart-seq2 to perform deep sequencing of the transcriptome. The advantage of LCM is the ability to obtain cells in situ without going through enzymatic digestions. In the process of isolating single cells most sequencing methods rely on the enzymatic disassembly of protein junctions between cells that has the disadvantage that

it can reduce the vitality of the cells and may also alter the molecular expression pattern of the cells (Nichterwitz et al., 2016). A flaw with our use of LCM was the 12-μm thickness of our frozen sections, resulting in the microtissue containing multiple cells, including a few glial cells surrounding a neuron. To reduce the interference from non-neuronal cells, the laser cutting was done close to the cell borders of neurons and later we removed some single cell samples with high glial cell markers. We determined by immunofluorescence staining that the target molecules were mainly expressed in neurons.

Conclusion and prospects

In addition to its role in gene epigenetic silencing (Cao and Zhang, 2004), Ezh2 can also bind to many important transcription factors to turn on gene expression (Jung et al., 2013). Among the molecules predicted by our IPA to act downstream of Ezh2 were those reported as transcription factors relating to PNI repair. For example, Atf3 promotes axonal regeneration by regulating regeneration-related gene clusters (Gey et al., 2016). Jun has been reported to mediate axonal regeneration by promoting nerve germination, lymphocyte recruitment, and microglia activation (Raivich et al., 2004). *Smad1* has been reported to inhibit axonal regeneration in DRG neurons after disrupted expression (Zou et al., 2009). Thus, we speculate that *Ezh2* may act in conjunction with these transcription factors to affect the regeneration of DRG neurons. In addition to acting in conjunction with transcription factors, other effectors of *Ezh2* in DRG neurons need to be explored. Among our predicted downstream factors, we have found that inhibition of *Bcl2l11* and *Ptgs2* can inhibit neuronal apoptosis (Xiao et al., 2019; Li et al., 2020) and that they are down-regulated in expression after nerve injury.

Therefore, whether *Ezh2* can enhance neuron survival after axonal injury through those molecules and thus synergistically promote axonal injury repair should also be investigated further.

There are so many predicted upstream regulators of Ezh2, for example, CASR was reported to promote axon and dendrite growth in developing neurons (Vizard et al., 2015; Markworth et al., 2019). MYC has also been reported to play a facilitating role in neuronal axon regeneration after PNI or optic nerve injury (Belin et al., 2015; Shin et al., 2021). In addition, downstream of Ezh2, we found various types of molecules including transcription factors, cytokines and enzymes, among which transcription factors ATF3 and SMAD1 have been reported to promote axonal injury repair (Zou et al., 2009; Gey et al., 2016). Some other molecules, including CDKN1A (Tomita et al., 2006), CCl2 (Zigmond and Echevarria, 2019) and SOCS3 (Gallaheret al., 2018), have been reported to participate in axonal damage repair. Among them, we identified a post-injury immediate-early gene *Myc*, a molecule that is classically up-regulated in expression after PNI and whose overexpression promotes axonal regeneration of the injured optic nerve (Belin et al., 2015). It has been reported that MYC was able to bind to the promoters of *Jun*, *Atf3*, and *Sparr1* of regeneration associated genes (RAGs) after pre-injury of peripheral nerve conditions and that MYC was up-regulated earlier than RAGs (Shin et al., 2021). In addition, it has been found that MYC can directly bind to the promoter of *Ezh2* to turn on the transcription of *Ezh2* (Koh et al., 2011). Ezh2 can also be recruited to the promoter of a gene *MYC* dependent, and the two combine to jointly regulate gene expression (Zhao et al., 2013). Our data showed that *Myc* expression is also up-regulated in DRG neurons after sciatic nerve injury, and it is likely that *Ezh2* is regulated by *Myc* and thus its expression is up-regulated. For the molecules which are downstream of *Ezh2*, a previous study found that Klf4 was a highly methylated state after 7 days of peripheral nerve injury treatment (Shin et al., 2020), and the knockdown of Klf4 in turn promoted the regeneration of optic nerve axons. Thus, future investigations should address how *Ezh2* works in promoting axon regeneration. In addition, future studies are needed to determine whether *Ezh2* turns on the expression of downstream RAGs by directly binding transcription factors such as ATF3, JUN, and SMAD1, turns off the expression of regeneration repressors by methylation, or whether both approaches work together.

Acknowledgments: *We thank Shu-Hai Yang, Nantong University, China for assistance in preparation of the manuscript.*
Author contributions: *Study concept and design: TTG, LLZ, XSG, SLZ; manuscript implementation: TTG, LLZ; data analysis: TTG, LLZ; providing reagents/materials/analysis tools: YZ, WXH, TZ; writing manuscript: TTG, LLZ, SLZ. All authors have read and approved the final manuscript.*
Conflicts of interest: *The authors declare no conflicts of interest.*
Editor note: XSG is an Editorial Board member of Neural Regeneration Research. He was blinded from reviewing or making decisions on the manuscript. The article was subject to the journal's standard procedures, with peer review handled independently of this Editorial Board member and his research groups.
Financial support: *This study was supported by the National Key Basic Research Program of China, No. 2017YFA0104701 (to XSG); the National Natural Science Foundation of China, No. 31730031(to XSG), 81870975 (to SLZ); Priority Academic Program Development of Jiangsu Higher Education Institutions (PAPD) (to XSG); the Natural Science Foundation of Jiangsu Province, No. BK20202013 (to XSG). The funding sources had no role in study conception and design, data analysis or interpretation, paper writing or decision to submit this paper for publication.*
Institutional review board statement: *All the experimental procedures involving animals were ethically approved by the Administration Committee of Experimental Animals of Jiangsu Province of China (approval No. S20191201-201) on March 21, 2019 and were used in accordance with Institutional Animal Care guidelines of Nantong University. The experimental procedure followed the United States National Institutes of Health Guide for the Care and Use of Laboratory Animals (NIH Publication No. 85-23, revised 1996).*
Copyright license agreement: *The Copyright License Agreement has been signed by all authors before publication.*
Data sharing statement: *Datasets analyzed during the current study are available from the corresponding author on reasonable request.*
Plagiarism check: *Checked twice by iThenticate.*
Peer review: *Externally peer reviewed.*

References

Belin S, Nawabi H, Wang C, Tang S, Latremoliere A, Warren P, Schorle H, Uncu C, Woolf CJ, He Z, Steen JA (2015) Injury-induced decline of intrinsic regenerative ability revealed by quantitative proteomics. Neuron 86:1000-1014.

Cao R, Zhang Y (2004) The functions of E(Z)/Ezh2-mediated methylation of lysine 27 in histone H3. Curr Opin Genet Dev 14:155-164.

Christie KJ, Webber CA, Martinez JA, Singh B, Zochodne DW (2010) PTEN inhibition to facilitate intrinsic regenerative outgrowth of adult peripheral axons. J Neurosci 30:9306-9315.

Chu W, Zhang X, Qi L, Fu Y, Wang P, Zhao W, Du J, Zhang J, Zhan J, Wang Y, Zhu WG, Yu Y, Zhang H (2020) The EZH2-PHACTR2-AS1-ribosome axis induces genomic instability and promotes growth and metastasis in breast cancer. Cancer Res 80:2737-2750.

Dudakovic A, Camilleri ET, Paradise CR, Samsonraj RM, Gluscevic M, Paggi CA, Begun DL, Khani F, Pichurin O, Ahmed FS, Elsayed R, Elsalanty M, McGee-Lawrence ME, Karperien M, Riester SM, Thaler R, Westendorf JJ, van Wijnen AJ (2018) Enhancer of zeste homolog 2 (Ezh2) controls bone formation and cell cycle progression during osteogenesis in mice. J Biol Chem 293:12894-12907.

Fischer D (2017) Hyper-IL-6: a potent and efficacious stimulator of RGC regeneration. Eye (Lond) 31:173-178.

Gan L, Xu M, Hua R, Tan C, Zhang J, Gong Y, Wu Z, Weng W, Sheng W, Guo W (2018) The polycomb group protein Ezh2 induces epithelial-mesenchymal transition and pluripotent phenotype of gastric cancer cells by binding to PTEN promoter. J Hematol Oncol 11:9.

Gey M, Wanner R, Schilling C, Pedro MT, Sinske D, Knöll B (2016) Atf3 mutant mice show reduced axon regeneration and impaired regeneration-associated gene induction after peripheral nerve injury. Open Biol 6:160091.
Gu XK, Li XR, Lu ML, Xu H (2020) Lithium promotes proliferation and suppresses migration of Schwann cells. Neural Regen Res 15:1955-1961.
Haberberger RV, Barry C, Matusica D (2020) Immortalized dorsal root ganglion neuron cell lines. Front Cell Neurosci 14:184.
Heinen A, Tzekova N, Graffmann N, Torres KJ, Uhrberg M, Hartung HP, Küry P (2012) Histone methyltransferase enhancer of zeste homolog 2 regulates Schwann cell differentiation. Glia 60:1696-1708.
Hu G, Huang K, Hu Y, Du G, Xue Z, Zhu X, Fan G (2016) Single-cell RNA-seq reveals distinct injury responses in different types of DRG sensory neurons. Sci Rep 6:31851.
Hussain G, Wang J, Rasul A, Anwar H, Qasim M, Zafar S, Aziz N, Razzaq A, Hussain R, de Aguilar JG, Sun T (2020) Current status of therapeutic approaches against peripheral nerve injuries: a detailed story from injury to recovery. Int J Biol Sci 16:116-134.
Julius MH, Masuda T, Herzenberg LA (1972) Demonstration that antigen-binding cells are precursors of antibody-producing cells after purification with a fluorescence-activated cell sorter. Proc Natl Acad Sci U S A 69:1934-1938.
Jung HY, Jun S, Lee M, Kim HC, Wang X, Ji H, McCrea PD, Park JI (2013) PAF and Ezh2 induce Wnt/β-catenin signaling hyperactivation. Mol Cell 52:193-205.
Kalender AM, Dogan A, Bakan V, Yildiz H, Gokalp MA, Kalender M (2009) Effect of Zofenopril on regeneration of sciatic nerve crush injury in a rat model. J Brachial Plex Peripher Nerve Inj 4:6.
Kampanis V, Tolou-Dabbaghian B, Zhou L, Roth W, Puttagunta R (2020) Cyclic stretch of either PNS or CNS located nerves can stimulate neurite outgrowth. Cells 10:32.
Koh CM, Iwata T, Zheng Q, Bethel C, Yegnasubramanian S, De Marzo AM (2011) Myc enforces overexpression of Ezh2 in early prostatic neoplasia via transcriptional and post-transcriptional mechanisms. Oncotarget 2:669-683.
Krill L, Deng W, Eskander R, Mutch D, Zweizig S, Hoang B, Ioffe O, Randall L, Lankes H, Miller DS, Birrer M (2020) Overexpression of enhance of Zeste homolog 2 (Ezh2) in endometrial carcinoma: an NRG oncology/gynecologic oncology group study. Gynecol Oncol 156:423-429.
Li C, Liu SY, Pi W, Zhang PX (2021) Cortical plasticity and nerve regeneration after peripheral nerve injury. Neural Regen Res 16:1518-1523.
Li CL, Li KC, Wu D, Chen Y, Luo H, Zhao JR, Wang SS, Sun MM, Lu YJ, Zhong YQ, Hu XY, Hou R, Zhou BB, Bao L, Xiao HS, Zhang X (2016) Somatosensory neuron types identified by high-coverage single-cell RNA-sequencing and functional heterogeneity. Cell Res 26:83-102.
Li J, Li D, Zhou H, Wu G, He Z, Liao W, Li Y, Zhi Y (2020) MicroRNA-338-5p alleviates neuronal apoptosis via directly targeting BCL2L11 in APP/PS1 mice. Aging (Albany NY) 12:20728-20742.
Mallen-St Clair J, Soydaner-Azeloglu R, Lee KE, Taylor L, Livanos A, Pylayeva-Gupta Y, Miller G, Margueron R, Reinberg D, Bar-Sagi D (2012) Ezh2 couples pancreatic regeneration to neoplastic progression. Genes Dev 26:439-444.
Markworth R, Adolfs Y, Dambeck V, Steinbeck LM, Lizé M, Pasterkamp RJ, Bähr M, Dean C, Burk K (2019) Sensory axon growth requires spatiotemporal integration of CaSR and TrkB signaling. J Neurosci 39:5842-5860.
Nichterwitz S, Chen G, Aguila Benitez J, Yilmaz M, Storvall H, Cao M, Sandberg R, Deng Q, Hedlund E (2016) Laser capture microscopy coupled with Smart-seq2 for precise spatial transcriptomic profiling. Nat Commun 7:12139.
Noble J, Munro CA, Prasad VS, Midha R (1998) Analysis of upper and lower extremity peripheral nerve injuries in a population of patients with multiple injuries. J Trauma 45:116-122.
Oppenheim RW (1991) Cell death during development of the nervous system. Annu Rev Neurosci 14:453-501.
Platika D, Boulos MH, Baizer L, Fishman MC (1985) Neuronal traits of clonal cell lines derived by fusion of dorsal root ganglia neurons with neuroblastoma cells. Proc Natl Acad Sci U S A 82:3499-3503.
Pope JE, Deer TR, Kramer J (2013) A systematic review: current and future directions of dorsal root ganglion therapeutics to treat chronic pain. Pain Med 14:1477-1496.
Poplawski G, Ishikawa T, Brifault C, Lee-Kubli C, Regestam R, Henry KW, Shiga Y, Kwon H, Ohtori S, Gonias SL, Campana WM (2018) Schwann cells regulate sensory neuron gene expression before and after peripheral nerve injury. Glia 66:1577-1590.
Raivich G, Bohatschek M, Da Costa C, Iwata O, Galiano M, Hristova M, Nateri AS, Makwana M, Riera-Sans L, Wolfer DP, Lipp HP, Aguzzi A, Wagner EF, Behrens A (2004) The AP-1 transcription factor c-Jun is required for efficient axonal regeneration. Neuron 43:57-67.
Renthal W, Tochitsky I, Yang L, Cheng YC, Li E, Kawaguchi R, Geschwind DH, Woolf CJ (2020) Transcriptional reprogramming of distinct peripheral sensory neuron subtypes after axonal injury. Neuron 108:128-144.e129.
Rugiero F, Wood JN (2009) The mechanosensitive cell line ND-C does not express functional thermoTRP channels. Neuropharmacology 56:1138-1146.
Shin HY, Kim K, Kwon MJ, Oh YJ, Kim EH, Kim HS, Hong CP, Lee JH, Lee K, Kim BG (2020) Alteration in global DNA methylation status following preconditioning injury influences axon growth competence of the sensory neurons. Exp Neurol 326:113177.
Shin HY, Kwon MJ, Lee EM, Kim K, Oh YJ, Kim HS, Hwang DH, Kim BG (2021) Role of Myc proto-oncogene as a transcriptional hub to regulate the expression of regeneration-associated genes following preconditioning peripheral nerve injury. J Neurosci 41:446-460.
Stupack J, Xiong XP, Jiang LL, Zhang T, Zhou L, Campos A, Ranscht B, Mobley W, Pasquale EB, Xu H, Huang TY (2020) Soluble SORLA enhances neurite outgrowth and regeneration through activation of the EGF receptor/ERK signaling axis. J Neurosci 40:5908-5921.
Thier M, März P, Otten U, Weis J, Rose-John S (1999) Interleukin-6 (IL-6) and its soluble receptor support survival of sensory neurons. J Neurosci Res 55:411-422.
Tomita K, Kubo T, Matsuda K, Madura T, Yano K, Fujiwara T, Tanaka H, Tohyama M, Hosokawa K (2006) p21Cip1/WAF1 regulates radial axon growth and enhances motor functional recovery in the injured peripheral nervous system. Brain Res 1081:44-52.
Tran NM, Shekhar K, Whitney IE, Jacobi A, Benhar I, Hong G, Yan W, Adiconis X, Arnold ME, Lee JM, Levin JZ, Lin D, Wang C, Lieber CM, Regev A, He Z, Sanes JR (2019) Single-cell profiles of retinal ganglion cells differing in resilience to injury reveal neuroprotective genes. Neuron 104:1039-1055.e1012.
Tsou PS, Campbell P, Amin MA, Coit P, Miller S, Fox DA, Khanna D, Sawalha AH (2019) Inhibition of Ezh2 prevents fibrosis and restores normal angiogenesis in scleroderma. Proc Natl Acad Sci U S A 116:3695-3702.
Usoskin D, Furlan A, Islam S, Abdo H, Lönnerberg P, Lou D, Hjerling-Leffler J, Haeggström J, Kharchenko O, Kharchenko PV, Linnarsson S, Ernfors P (2015) Unbiased classification of sensory neuron types by large-scale single-cell RNA sequencing. Nat Neurosci 18:145-153.
Utada AS, Lorenceau E, Link DR, Kaplan PD, Stone HA, Weitz DA (2005) Monodisperse double emulsions generated from a microcapillary device. Science 308:537-541.
Vizard TN, Newton M, Howard L, Wyatt S, Davies AM (2015) ERK signaling mediates CaSR-promoted axon growth. Neurosci Lett 603:77-83.
Wang D, Chen Y, Liu M, Cao Q, Wang Q, Zhou S, Wang Y, Mao S, Gu X, Luo Z, Yu B (2020) The long noncoding RNA Arrl1 inhibits neurite outgrowth by functioning as a competing endogenous RNA during neuronal regeneration in rats. J Biol Chem 295:8374-8386.
Wever I, von Oerthel L, Wagemans C, Smidt MP (2018) Ezh2 Influences mdDA neuronal differentiation, maintenance and survival. Front Mol Neurosci 11:491.
Whitesides GM (2006) The origins and the future of microfluidics. Nature 442:368-373.
Wood JN, Bevan SJ, Coote PR, Dunn PM, Harmar A, Hogan P, Latchman DS, Morrison C, Rougon G, Theveniau M (1990) Novel cell lines display properties of nociceptive sensory neurons. Proc Biol Sci 241:187-194.
Xiao X, Jiang Y, Liang W, Wang Y, Cao S, Yan H, Gao L, Zhang L (2019) miR-212-5p attenuates ferroptotic neuronal death after traumatic brain injury by targeting Ptgs2. Mol brain 12:78.
Yadav R, Weng HR (2017) Ezh2 regulates spinal neuroinflammation in rats with neuropathic pain. Neuroscience 349:106-117.
Yang YJ, Xia B, Gao JB, Li SY, Ma T, Huang JH, Luo ZJ (2020) Cell culture supernatant of olfactory ensheathing cells promotes nerve regeneration after peripheral nerve injury in rats. Zhongguo Zuzhi Gongcheng Yanjiu 24:3035-3041.
Zemel BM, Ritter DM, Covarrubias M, Muqeem T (2018) A-Type K(V) Channels in dorsal root ganglion neurons: diversity, function, and dysfunction. Front Mol Neurosci 11:253.
Zhao X, Lwin T, Zhang X, Huang A, Wang J, Marquez VE, Chen-Kiang S, Dalton WS, Sotomayor E, Tao J (2013) Disruption of the MYC-miRNA-Ezh2 loop to suppress aggressive B-cell lymphoma survival and clonogenicity. Leukemia 27:2341-2350.
Zigmond RE, Echevarria FD (2019) Macrophage biology in the peripheral nervous system after injury. Prog Neurobiol 173:102-121.
Zingg D, Debbache J, Schaefer SM, Tuncer E, Frommel SC, Cheng P, Arenas-Ramirez N, Haeusel J, Zhang Y, Bonalli M, McCabe MT, Creasy CL, Levesque MP, Boyman O, Santoro R, Shakhova O, Dummer R, Sommer L (2015) The epigenetic modifier Ezh2 controls melanoma growth and metastasis through silencing of distinct tumour suppressors. Nat Commun 6:6051.
Zou H, Ho C, Wong K, Tessier-Lavigne M (2009) Axotomy-induced Smad1 activation promotes axonal growth in adult sensory neurons. J Neurosci 29:7116-7123.

C-Editor: Zhao M; S-Editors: Wang J, Li CH; L-Editors: Dawes ED, Song LP; T-Editor: Jia Y